Theoretical Investigation of Electron-Deficient and/or Paramagnetic Complexes Composed of the Cp*Fe(dppe) Unit and of Related Compounds

Karine Costuas and Jean-Yves Saillard*

LCSIM UMR 6511, Université de Rennes 1, 35042 Rennes Cedex, France

Received March 17, 1999

DFT calculations performed on the 16-electron $[Cp^*Fe(dppe)]^+$ complex found a triplet ground state with a small singlet−triplet separation, in agreement with experiment. The reason for this lies in the fact that, although the HOMO−LUMO gap of the complex is small, its second-order Jahn−Teller instability with respect to iron pyramidalization is weak. Calculations on a series of 16-electron models of the type $CpML_2$ (L = σ-donor or π-acceptor) found similarly a small singlet−triplet separation, with a low-spin ground state slightly favored in the case of L = π-acceptor. With L = π-donor the LUMO is strongly destabilized, leading to a highly favored singlet state. The 17- and 18-electron $[Cp^*Fe(dppe)]^{0/-}$ complexes were also modelized as well as other $CpML_2$-type models. When L = π-donor, the destabilization of the HOMO leads to a small HOMO−LUMO gap, with no Jahn−Teller instability. As a consequence, the computed singlet−triplet separation is very small, in full agreement with experimental data. Eighteen-electron complexes resulting from the association of the $[Cp^*Fe(dppe)]^+$ unit with water, acetone, or triflate have also been investigated. Although the Fe−O bond is weak in these complexes, the low-spin state is always found to be more stable than the high-spin state by more than 0.5 eV, at variance with the reported magnetic behavior of two of them.

Introduction

Stable isolable molecular compounds most often satisfy the closed-shell requirement, i.e. are diamagnetic and exhibit a significant HOMO/LUMO gap separating the occupied bonding and nonbonding orbitals from the vacant antibonding orbitals.[1] Assuming a localized bonding scheme, the effective atomic number (EAN) rule can be easily derived from the closed-shell requirement principle. In organometallic chemistry, this rule, usually called the 18-electron rule, is generally considered as a major criterion for stability[1] and is satisfied for most of the isolable complexes. However, for several years an increasing number of simple complexes having more or less than 18 electrons in the transition-metal environment have been characterized.[2−10] Various theoretical treatments have been used to understand the structure and the stability of these electron-rich and electron-poor molecules.[2,3d−f,t,6c,7d,8,12−17] Moreover, 18-electron paramagnetic complexes, thus not satisfying the closed-shell requirement, have also been reported.[5,6f,9b,18] Recently, a series of paramagnetic electron-poor and 18-electron species, all containing the Cp*Fe(dppe) (Cp* = η^5-C_5Me_5; dppe = $Ph_2PCH_2CH_2PPh_2$) moiety, have been characterized in the group of Lapinte and Hamon.[6f,18a] This paper investigates the electronic structure of these complexes and of various related species with the help of density functional theory (DFT) calculations, to rationalize their stability, structure, and properties. To

(1) Albright, T. A.; Burdett, J. K.; Wangbo, M.-H. *Orbital Interactions in Chemistry*; John Wiley: New York, 1985.

(2) For leading references see for example (and references therein): (a) Tyler, R. D. *Acc. Chem. Res.* **1991**, *24*, 325. (b) Astruc, D. *Electron Transfer and Radical Processes in Transition-Metal Chemistry*; VCH: New York, 1995. (c) Poli, R. *Chem. Rev.* **1996**, *96*, 2135. (d) Poli, R. *Acc. Chem. Res.* **1997**, *30*, 494. (e) Baird, M. C. *Chem. Rev.* **1988**, *88*, 1217.

(3) Selected references for characterized organometallic mononuclear complexes not satisfying the 18-electron rule: (a) Astruc, D.; Hamon, J. R.. Althoff, G.; Román, E.; Batail, P.; Michaud, P. *J. Am. Chem. Soc.* **1979**, *101*, 1, 5545. (b) Madonic, A. M.; Astruc, D. *J. Am. Chem. Soc.* **1984**, *106*, 2437. (c) Lacoste, M.; Rabaâ, H.; Astruc, D.; Saillard, J.-Y.; Le Beuze, A.; Varret, F.; Ardoin, N. *J. Am. Chem. Soc.* **1990**, *112*, 9548. (d) Rabaâ H.; Lacoste, M.; Delville-Desbois, M.-H.; Ruiz, J.; Gloaguen, B.; Ardoin, N.; Astruc, D.; Le Beuze, A.; Saillard, J.-Y.; Linares, J.; Varret, F.; Dance, J.-M.; Marquestaut, E. *Organometallics* **1995**, *14*, 5078. (e) Delville-Desbois M.-H.; Mross, S.; Astruc, D.; Linares, J.; Varet, F.; Rabaâ, H.; Le Beuze, A.; Saillard, J.-Y.; Cowley, A. H. *J. Am. Chem. Soc.* **1996**, *118*, 4133. (f) Ruiz, J.; Ogliaro, F.; Saillard, J.-Y.; Halet, J.-F.; Varret, F.; Astruc, D. *J. Am. Chem. Soc.* **1998**, *120*, 11693. (g) Michaud, P.; Mariot, J.-P.; Varret, F.; Astruc, D. *J. Chem. Soc. Chem. Commun.* **1982**, 1383. (h) Michaud, P.; Astruc, D.; Ammeter, J. H. *J. Am. Chem. Soc.* **1982**, *104*, 3754. (i) Connelly, N. G.; Geiger, W. E.; Lane, G. A.; Raven, S. J.; Rieger, P. H. *J. Am. Chem. Soc.* **1986**, *108*, 6219. (j) Collins, J. E.; Castellani, M. P.; Rheingold, A. L.; Miller, E. J.; Geiger, W. E.; Rieger A. L.; Rieger, P. H. *Organometallics* **1995**, *14*, 1232. (k) Hays, M. L.; Burkey, D. J.; Overby, J. S.; Hanusa, T. P.; Sellers, S. P.; Yee, G. T.; Young, V. G., Jr. *Organometallics* **1998**, *17*, 5521. (l) Thomas, B. J.; Kyun Noh, S.; Schulte, G. K.; Sendlinger, S. C.; Theopold, K. H. *J. Am. Chem. Soc.* **1991**, *113*, 893. (m) Bhandari, G.; Kim, Y.; McFarland, J. M.; Rheingold, A. L.; Theopold K. H. *Organometallics* **1995**, *14*, 738. (n) Liang, Y.; Yap, G. P. A.; Rheingold, A. L.; Theoplod, K. H. *Organometallics* **1996**, *15*, 5284. (o) White, P. A.; Calabrese, J.; Theopold, K. H. *Organometallics* **1996**, *15*, 5473. (p) Wang, X.; Liable-Sands, L. M.; Manson, J. L.; Rheingold, A. L.; Miller, J. S. *J. Chem. Soc., Chem. Commun.* **1996**, 1979. (q) Herberich, G. E.; Klein, W.; Spaniol, T. P. *Organometallics* **1993**, *12*, 2660. (r) Field, L. D.; Hambley, T. W.; He, T.; Humphrey, P. A.; Lindall, C. M.; Masters, A. F. *Aust. J. Chem.* **1996**, *49*, 889. (s) Thompson, M. R.; Day, C. S.; Day, V. W.; Mink, R. I.; Muetterties, E. L. *J. Am. Chem. Soc.* **1980**, *102*, 2979. (t) Koelle, U.; Fuss, B.; Rajasekharan, M. V.; Ramakrishna, B. L.; Ammeter, J. H.; Böhm, M. C. *J. Am. Chem. Soc.* **1984**, *106*, 4152. (u) Koelle, U.; Khouzami, F. *Angew. Chem., Int. Ed. Engl.* **1980**, *19*, 640. (v) Samuel, E.; Caurant, D.; Gourier, D.; Elschenbroich, Ch.; Agbaria, K. *J. Am. Chem. Soc.* **1998**, *120*, 8088.

10.1021/om990191i CCC: $18.00
Publication on Web 06/21/1999

reduce computational effort, the Cp*Fe(dppe) fragment has been modelized in several of these complexes by the smaller CpFe(dpe) (Cp = η^5-C_5H_5; dpe = $H_2PCH_2CH_2$-PH_2) unit. Details of the calculations are given below.

Computational Details

DFT calculations[19] were carried out on each compound using the Amsterdam Density Functional (ADF) program.[20] Electron correlation was treated within the local density approximation (LDA) in the Vosko−Wilk−Nusair parametrization.[21] Becke's nonlocal corrections[22] to the exchange energy and Perdew's nonlocal corrections[23] to the correlation energy were added. The numerical integration procedure applied for the calculations was developed by te Velde et al.[19c] A triple-ζ Slater-type orbital (STO) basis set was used for describing valence metal orbitals (3d and 4s for Fe, Co, Ni; 4d and 5s for Ru) augmented with a single-ζ polarization function (4p for Fe, Co, Ni; 5p for Ru). A frozen-core approximation was used to treat the core shells of metals.[19a] A double-ζ STO basis set was employed for H 1s, C 2s and 2p, O 2s and 2p, F 2s and 2p, P 3s and 3p, Cl 3s and 3p extended with a single-ζ polarization function 2p and 3d respectively for H and C, O, F, Cl, and P. A frozen-core approximation was used to treat the core electrons of C, O, F, Cl, and P. Full geometry optimizations (assuming C_1 symmetry) were carried out on $[CpFe(dpe)]^+$, $[Cp^*Fe(dpe)]^+$, $[CpFe(dppe)]^+$, $[Cp^*Fe(dppe)]^+$, [CpFe(dpe)], $[CpFe(dpe)(OH_2)]^+$, $[CpFe(dpe)(OCMe_2)]^+$, $[Cp^*Fe(dpe)(OCMe_2)]^+$, $[Cp^*Fe(dppe)(OCMe_2)]^+$, $[CpFe(dpe)(OSO_2CF_3)]$, [CpRu(acac)], $[CpCo(acac)]^+$, [CpCo(acac)], [CpNi(acac)], and [Cp*Ni(acac)] for their two lowest spin states. Single-point calculations have also been performed on $[CpFe(dpe)]^+$, [CpFe(dpe)], $[CpFe(dpe)(OH_2)]^+$, $[CpFe(dpe)(OCMe_2)]^+$, $[CpFe(dpe)(OSO_2CF_3)]$, assuming the X-ray structures of $[Cp^*Fe(dppe)]^+$,[6f] [Cp*Fe(dppe)],[6f] $[Cp^*Fe(dppe)(OH_2)]^+$,[6f] $[Cp^*Fe(dppe)(OCMe_2)]^+$,[18a] $[Cp^*Fe(dppe)(OSO_2CF_3)]$,[18b] respectively and in which the methyl and phenyl groups were replaced by hydrogen atoms (C−H = 1.09 Å; P−H = 1.42 Å) without changing the corresponding bond angles. Full geometry optimizations were also carried out on the high-spin and low-spin configurations of the $[CpFe(dpe)]^-$, $[CpFe(H)_2]^-$, $[CpFe(CO)_2]^+$, $[Cp^*Fe(PH_3)_2]^+$, $[CpNi(Cl)_2]$ models. The C_1 symmetry was considered for the former and the C_s symmetry for the others. All the geometry optimizations were performed using the analytical gradient method implemented by Verluis and Ziegler.[24] Spin-unrestricted calculations were performed for all the considered open-shell systems.

The 16-, 17-, and 18-Electron $[CpFe(dpe)]^{+,0,-}$ Series

The $[Cp^*Fe(dppe)]^+$ and [Cp*Fe(dppe)] complexes have been structurally characterized by X-ray diffraction.[6f] Their major structural data are given in Table 1. In the 16-electron cation, the PFeP plane is almost perfectly perpendicular to the C_5 ring (α = Cp(centroid)−M−P_2(centroid) =175°), while in the neutral 17-electron species, the angle between the two planes is α = 167°, a value intermediate between 180° and the one corresponding to an ideal pseudo-octahedral ML_5 coordination mode around the iron atom (144.7°). As expected, [Cp*Fe(dppe)] is paramagnetic with an effective magnetic moment μ_{eff} = 1.5 μ_B. The 16-electron cation is also paramagnetic (μ_{eff} = 3.3 μ_B), suggesting two unpaired electrons.[6f] The 16-electron cation $[Cp^*Fe(dippe)]^+$ (dippe = $(^iPr)_2PCH_2CH_2P(^iPr)_2$) has also been isolated.[9b] Its molecular structure is very similar to that of $[Cp^*Fe(dppe)]^+$ (see Table 1). It is also paramagnetic with a reported μ_{eff} of 3.8 μ_B.[9b]

The electronic structure of 16-electron $CpML_2$ complexes has been investigated in detail by Hofmann and co-workers.[13] According to their most recent extended Hückel theory (EHT) and DFT investigation, the orthogonality between the Cp and LFeL planes (i.e., α = Cp(centroid)−M−L_2(centroid) = 180°) should be favored when the L ligands are σ-donors and π-donors. The pyramidalization of the metal center (α < 180°) is favored by π-acceptor ligands, especially if they are also strong σ-donors.[13c] Similar conclusions were reached independently by Eisenstein and co-workers, who focused their EHT investigation on systems containing π-donor ligands.[15b] They also found that pyramidalization is favored if only one of the two L ligands is a π-donor. However, all these authors considered only

(4) (a) Kölle, U.; Kossakowski, J.; Raabe, G. *Angew. Chem., Int. Ed. Engl.* **1990**, *29*, 773. (b) Smith, M. E.; Hollander, F. J.; Andersen, R. A. *Angew. Chem., Int. Ed. Engl.* **1993**, *32*, 1294.
(5) Smith, M. E.; Andersen, R. A. *J. Am. Chem. Soc.* **1996**, *118*, 11119.
(6) (a) Guerchais, V.; Lapinte, C. *J. Chem. Soc., Chem. Commun.* **1986**, 663. (b) Roger, C.; Toupet, L.; Lapinte, C. *J. Chem. Soc., Chem. Commun.* **1988**, 713. (c) Roger, C.; Hamon, P.; Toupet, L.; Rabaâ, H.; Saillard, J.-Y.; Lapinte, C. *Organometallics* **1991**, *10*, 1045. (d) Hamon, P.; Toupet, L.; Hamon, J.-R.; Lapinte, C. *Organometallics* **1992**, *11*, 1429. (e) Connelly, N. G.; Gamasa, M. P.; Gimeno, J.; Lapinte, C.; Lastra, E.; Maher, J. P.; Le Narvor, N.; Rieger, P. H.; Rieger, A. L. *J. Chem. Soc., Dalton Trans.* **1993**, 2575. (f) Hamon, P.; Toupet, L.; Hamon, J.-R.; Lapinte, C. *Organometallics* **1996**, *15*, 10.
(7) (a) Abugideiri, F.; Keogh, D. W.; Poli, R. *J. Chem. Soc., Chem. Commun.* **1994**, 2317. (b) Abugideiri, F.; Fettinger, J. C.; Keogh, D. W.; Poli, R. *Organometallics* **1996**, *15*, 4407. (c) Mattamana, S. P.; Poli, R. *Organometallics* **1997**, *16*, 2427. (d) Poli, R.; Quadrelli, E. A. *New. J. Chem.* **1998**, *22*, 435.
(8) Bleeke, J. R.; Wittenbrink, R. J.; Clayton, T. W., Jr.; Chiang, H. Y. *J. Am. Chem. Soc.* **1990**, *112*, 6539.
(9) (a) Jiménez Tenorio, M.; Puerta, M. C.; Valerga, P. *Organometallics* **1994**, *13*, 3330. (b) de la Jara Leal, A.; Jiménez Tenorio, M.; Puerta, M. C.; Valerga, P. *Organometallics* **1995**, *14*, 3839.
(10) (a) Diaz, C.; Arrancibia, A. *Polyhedron* **1994**, *13*, 117. (b) Diaz, C.; Yutronik, N. *Polyhedron* **1996**, *15*, 997. (c) Diaz, C.; Araya, E.; Ana, M. A. S. *Polyhedron* **1998**, *17*, 2225. (d) Diaz, C.; LaTorre, R. *Bol. Soc. Chil. Quim.* **1992**, *37*, 211.
(11) Sellmann, D.; Kleinschmidt, E. *J. Organomet. Chem.* **1977**, *140*, 211.
(12) (a) Braden, D. A.; Tyler, D. R. *J. Am. Chem. Soc.* **1998**, *120*, 942. (b) Campbell, J. M.; Martel, A. A.; Chen, S.-P.; Waller, I. M. *J. Am. Chem. Soc.* **1997**, *119*, 4678.
(13) (a) Hofmann, P. *Angew. Chem., Int. Ed. Engl.* **1977**, *16*, 536. (b) Hofmann, P.; Padmanabhan, P. M. *Organometallics* **1983**, *2*, 1273. (c) Ward, T. R.; Schafer, O.; Daul, C.; Hofmann, P. *Organometallics* **1997**, *16*, 3207.
(14) (a) El-Idrissi Rachidi, I.; Eisenstein, O.; Jean, Y. *New J. Chem.* **1990**, *14*, 671. (b) Riehl, J.-F.; Jean, Y.; Eisenstein, O.; Pélissier, M. *Organometallics* **1992**, *11*, 729.
(15) (a) Bickford, C. C.; Johnson, T. J.; Davidson, E. R.; Caulton, K. G. *Inorg. Chem.* **1994**, *33*, 1080. (b) Johnson, T. J.; Folting, K.; Streib, W. E.; Martin, J. D.; Huffman, J. C.; Jackson, S. A.; Eisenstein, O.; Caulton, K. G. *Inorg. Chem.* **1995**, *34*, 488.
(16) (a) Keogh, D. W.; Poli, R. *J. Am. Chem. Soc.* **1997**, *119*, 2516. (b) Legzdins, P.; McNeil, W. S.; Smith, K. M.; Poli, R. *Organometallics* **1998**, *17*, 615. (c) Smith, K. M.; Poli, R.; Legzdins, P. *J. Chem. Soc., Chem. Commun.* **1998**, 1903.
(17) Yang, Y.; Asplund, M. C.; Kotz, K. T.; Wilkens, M. J.; Frei, H.; Harris, C. B. *J. Am. Chem. Soc.* **1998**, *120*, 10154.
(18) (a) Hamon, P.; Toupet, L.; Hamon, J.-R.; Lapinte, C. *J. Chem. Soc., Chem. Commun.* **1994**, 931. (b) Hamon, P.; Hamon, J.-R.; Lapinte, C. Personal communication.
(19) (a) Baerends, E. J.; Ellis, D. E.; Ros, P. *Chem. Phys.* **1973**, *2*, 41. (b) Baerends, E. J.; Ros, P. *Int. J. Quantum Chem.* **1978**, *S12*, 169. (c) Boerrigter, P. M.; te Velde, G.; Baerends, E. J. *Int. J. Quantum Chem.* **1988**, *33*, 87. (d) te Velde, G.; Baerends, E. J. *J. Comput. Phys.* **1992**, *99*, 84.
(20) Baerends E. J.; et al. *Amsterdam Density Functional (ADF) program*, version 2.3; Vrije Universiteit, Amsterdam, The Netherlands, 1997.
(21) Vosko, S. D.; Wilk, L.; Nusair, M. *Can. J. Chem.* **1990**, *58*, 1200.
(22) (a) Becke, A. D. *J. Chem. Phys.* 1**986**, *84*, 4524. (b) Becke, A. D. *Phys. Rev. A* **1988**, *38*, 3098.
(23) (a) Perdew, J. P. *Phys. Rev. B* **1986**, *33*, 8882. (b) Perdew, J. P. *Phys. Rev. B* **1986**, *34*, 7406.
(24) Verluis, L.; Ziegler, T. *J. Chem. Phys.* **1988**, *88*, 322.

Table 1. Major Experimental and Optimized Structural Data and Relative Energies for Various $CpML_2$ Species

		M−C (Å) average (range)	M−L (Å)	L−M−L (deg)	α (deg)	energy (eV)
$[CpFe(dpe)]^+$	expt[a]	2.13 (2.11−2.15)	2.26, 2.23	86	175	0.35 (T)[b]
	expt[c]	2.16 (2.13−1.19)	2.29, 2.29	87	176	
	S	2.10 (2.07−2.13)	2.23, 2.21	86	145	0.13
	T	2.18 (2.13−2.24)	2.27, 2.25	87	180	0.00
$[CpFe(dppe)]^+$	S	2.10 (2.07−2.12)	2.24, 2.22	87	154	0.19
	T	2.19 (2.15−2.23)	2.28, 2.25	87	177	0.00
$[Cp^*Fe(dpe)]^+$	S	2.10 (2.07−2.12)	2.24, 2.22	87	154	0.01
	T	2.17 (2.13−2.22)	2.27, 2.25	87	179	0.00
$[Cp^*Fe(dppe)]^+$	expt[a]	2.13 (2.11−2.15)	2.26, 2.23	86	175	
	S	2.11 (2.09−2.12)	2.29, 2.26	86	162	0.12
	T	2.19 (2.15−2.24)	2.28, 2.25	87	177	0.00
$[CpFe(dpe)]$	expt[d]	2.10 (2.09−2.12)	2.15, 2.13	87	167	0.30 (D)[b]
	D	2.15 (2.14−2.17)	2.16, 2.16	87	162	0.00
$[CpFe(dpe)]^-$	S	2.12 (2.11−2.15)	2.11, 2.12	86	174	0.00
	T	2.33 (2.31−2.38)	2.20, 2.20	88	161	0.49
$[CpFe(H)_2]^-$	S	2.08 (2.05−2.12)	1.58	89	174	0.60
	T	2.31 (2.20−2.44)	1.57	84	175	0.00
$[CpFe(PH_3)_2]^+$	S	2.09 (2.07−2.10)	2.26	99	154	0.14
	T	2.19 (2.15−2.26)	2.30	96	177	0.00
$[CpFe(CO)_2]^+$	S	2.12 (2.07−2.14)	1.83	94	143	0.00
	T	2.19 (2.15−2.30)	1.87	104	180	0.12
$[CpRu(acac)]$	expt[e]	2.13	2.11	85	144	
	S	2.19 (2.16−2.21)	2.08	90	176	0.00
	T	2.36 (2.32−2.46)	2.09	91	178	0.94
$[CpCo(acac)]^+$	S	2.09 (2.07−2.10)	1.85, 1.85	95	176	0.00
	T	2.21 (2.18−2.28)	1.88	98	173	0.49
$[CpCo(acac)]$	expt[f]	2.08 (2.05−2.09)	1.88, 1.89	95	177	
	D	2.14 (2.12−2.16)	1.89	96	174	0.00
$[Cp^*Ni(acac)]$	expt[g]	2.13 (2.06−2.20)	1.87, 1.88	98	177	
	S	2.19 (2.13−2.27)	1.90	99	176	0.00
	T	2.22 (2.17−2.24)	1.96	95	176	0.08
$[CpNi(acac)]$	S	2.20 (2.14−2.28)	1.89	98	174	0.00
	T	2.22 (2.21−2.24)	1.97	94	177	0.00
$[CpNi(Cl)_2]$	S	2.16 (2.14−2.17)	2.18	98	178	0.00
	T	2.23 (2.23−2.25)	2.20	106	175	0.22

[a] X-ray structure of $[Cp^*Fe(dppe)]^+$ (from ref 6f). [b] Single-point calculation (ground state) performed on the corresponding X-ray structure in which the methyl and phenyl groups were replaced by hydrogen atoms (C−H = 1.09 Å; P−H = 1.42 Å). [c] X-ray structure of $[Cp^*Fe(dippe)]^+$ (from ref 9b). [d] X-ray structure of $[Cp^*Fe(dppe)]$ (from ref 6f). [e] X-ray structure of $[Cp^*Ru(acac)]$ (from ref 4). [f] X-ray structure of $[Cp^*Co(acac)]$ (from ref 5). [g] X-ray structure of $[Cp^*Ni(acac)]$ (from ref 5).

diamagnetic systems. Very recently, Poli and co-workers published a DFT study of the singlet and triplet states of $[CpW(NO)(PH_3)]$.[16c] The singlet state was found pyramidalized, while the triplet state was not. The triplet state was found to be the most stable by 0.14 eV. Very similar results were obtained simultaneously by Harris et al. on $CpMn(CO)_2$ at the DFT and CASSCF-PT2 levels.[17]

The qualitative Walsh diagram corresponding to the variation of α from 180° to 145° is sketched in Figure 1 for a 16-electron $CpML_2$ system (based on EHT calculations on $[CpFe(CO)_2]^+$). When α = 180°, the pseudo-symmetry of the molecule is C_{2v}, while it is of C_s symmetry for α < 180°. In the pseudo-C_{2v} geometry, the HOMO is a_1 and the LUMO is b_1. In the pyramidalized C_s conformation, both HOMO and LUMO are of a′ symmetry and can interact and repel each other. As found on $[CpMn(CO)_2]$ by Hofmann a long time ago,[13a] pyramidalization enlarges the HOMO−LUMO gap and therefore is expected to stabilize somewhat the singlet state, although more recent work from this group[13c] (see above) suggests that pure σ-donor ligands have a HOMO−LUMO gap large enough to prevent this second-order Jahn−Teller distortion. On the other hand, the pseudo-C_{2v} geometry is expected to stabilize the triplet state.

The major results of the DFT-optimized geometries of the singlet and triplet states of $[CpFe(dpe)]^+$ are given

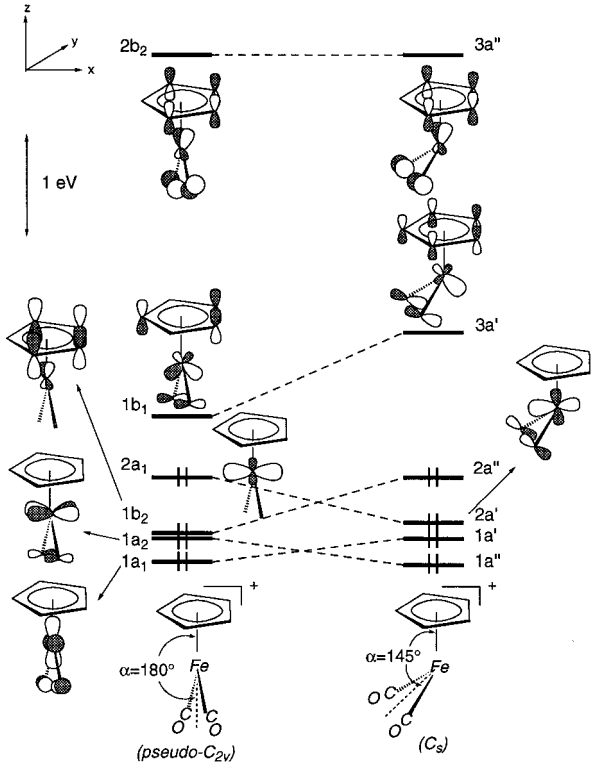

Figure 1. Qualitative Walsh diagram associated with the pyramidalization of $[CpFe(CO)_2]^+$.

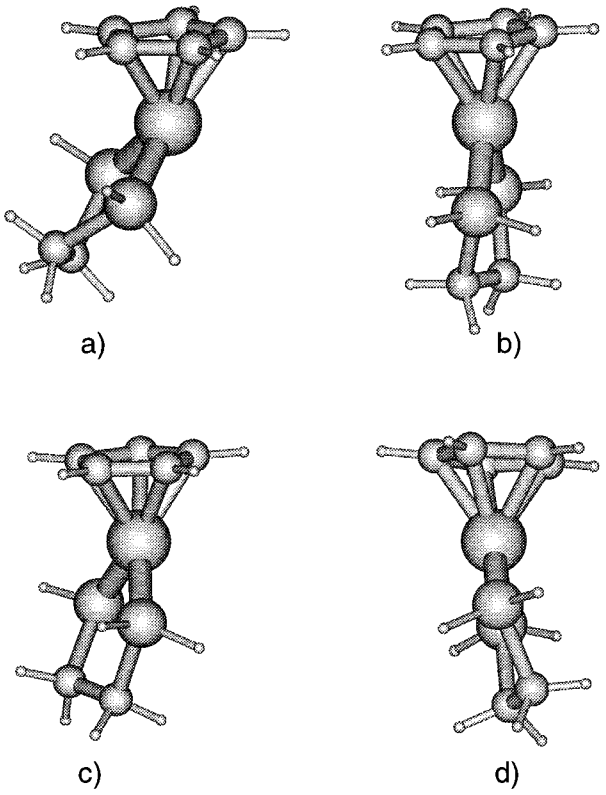

Figure 2. Optimized geometries of (a) $[CpFe(dpe)]^+$ ($S = 0$); (b) $[CpFe(dpe)]^+$ ($S = 1$); (c) [CpFe(dpe)] ($S = 1/2$); and (d) $[CpFe(dpe)]^-$ ($S = 0$). Plots were obtained by using the MOLDEN package (Schaftenaar, G., CAOS/CAMM Center Nijmegen, The Netherlands).

in Table 1. Both geometries are shown in Figure 2a,b. They differ mainly from their α angles. The singlet state is pyramidalized, with a α value close to the ideal pseudo-octahedral ML_5 coordination one. On the other hand, the triplet state has a pseudo-C_{2v} structure. In agreement with the paramagnetic behavior of $[Cp^*Fe(dppe)]^+$, the triplet state of the $[CpFe(dpe)]^+$ model is computed to be the ground state by 0.13 eV. This value is almost equal to that found by Poli and co-workers on the isoelectronic complex $[CpW(NO)(PH_3)]$.[16c] The optimized geometry of $[CpFe(dpe)]^+$ is close to the experimental molecular structures of $[Cp^*Fe(dppe)]^+$[6f] and $[Cp^*Fe(dippe)]^+$[9b] (Table 1). In particular, the α angles differ only by 4−5°, a value barely significant at our level of theory and modelization. Single-point calculations have also been performed on $[CpFe(dpe)]^+$, considering a molecular geometry derived from the X-ray structure of $[Cp^*Fe(dppe)]^+$[6f] (see Computational Details). Again, the triplet state is found to be the more stable, by 0.49 eV. The singlet state HOMO−LUMO gap computed for this close-to-C_{2v} geometry (0.20 eV) is much smaller that those found for the corresponding triplet state (2.07 and 1.05 eV for the α and β spins, respectively).

To evaluate the effect of modelizing Cp* by Cp and dppe by dpe, we have also performed full geometry optimizations on $[CpFe(dppe)]^+$, $[Cp^*Fe(dpe)]^+$, and $[Cp^*Fe(dppe)]^+$ (see Table 1). Substituting the diphosphine ligand in $[CpFe(dpe)]^+$ by dppe increases slightly the singlet−triplet separation, while substituting Cp by Cp* induces the opposite effect. As a result, the combination of both substitutions leads to a very small change in this energy difference (Table 1).

The existence of the 18-electron anion $[Cp^*Fe(dppe)]^-$ has been evidenced at low temperature by in situ trapping with methyl iodide, which gives $[Cp^*Fe(dppe)Me]$ in good yield.[18b] Adding two electrons to the Walsh diagram of Figure 1, one is led to predict that $[Cp^*Fe(dppe)]^-$ should be diamagnetic and adopt the pseudo-C_{2v} structure. Indeed, the $\alpha = 180°$ value provides the 18-electron system with its largest HOMO−LUMO gap. As a matter of fact, this conformation is known to be that of isoelectronic $CpML_2$ complexes, such as $[CpCo(CO)_2]$ for instance.[1,25] The $[CpFe(dpe)]^-$ 18-electron model was computed in both the singlet and triplet states. The major optimized structural parameters are reported in Table 1. As expected, the singlet state is found to be the most stable. It is slightly pyramidalized geometry ($\alpha = 174°$, see Figure 2c), while the triplet state is as pyramidalized as its neutral 17-electron parent (see below).

Having an electron configuration intermediate between those of the singlet states of $[CpFe(dpe)]^+$ and $[CpFe(dpe)]^-$, the 17-electron [CpFe(dpe)] complex adopts an α value intermediate between 145° and 174°, as shown in Table 1, which summarizes the major DFT results computed for [CpFe(dpe)]. This optimized geometry, shown in Figure 2d, is very similar to the experimental structure of the isoelectronic $[Cp^*Fe(dppe)]$ complex.[6f] Again, the optimized and experimental α angles differ by only 5° and are, as expected from the above qualitative considerations, close to the average of the values computed for the singlet and triplet states of the 16-electron parent. It is also close to the value found for the triplet state of $[CpFe(dpe)]^-$. This was expected, since adding an extra electron to the [CpFe(dpe)] b_2 LUMO cannot affect α, because this orbital is antisymmetrical with respect to the symmetry plane which is conserved upon pyramidalization. Single-point calculations on [CpFe(dpe)] assuming a molecular geometry derived from the X-ray structure of $[Cp^*Fe(dppe)]$[6f] lead to an energy only 0.30 eV higher than that corresponding to the full optimization. For this geometry, the quadruplet state was also computed and was found lying 1.79 eV above the doublet ground state.

Comparison with Other $CpML_2$ Systems

Sixteen-electron species. As said above, Hofmann and co-workers concluded from their most recent theoretical investigation that pure σ-donor ligands favor the existence of the Jahn−Teller stable pseudo-C_{2v} structure for the closed-shell 16-electron $CpML_2$ species.[13c] As a matter of fact, their DFT-optimized geometry of the $[CpFeH_2]^-$ model was found to adopt this conformation, a result apparently at variance with our calculations on the singlet state of $[CpFe(dpe)]^+$, which, despite the σ-donor nature of the diphosphine ligand, was found strongly pyramidalized (see above). We have also carried out calculations on $[CpFeH_2]^-$ and found similarly a pseudo-C_{2v} singlet state (see Table 1). Interestingly, though the pyramidalization is not favored, the corresponding HOMO−LUMO gap is small (0.47 eV). The

(25) (a) Byers, L. R.; Dahl, L. F. *Inorg. Chem.* **1980**, *19*, 277. (b) Albright, T. A.; Hoffmann, R. *Chem. Ber.* **1978**, *111*, 1578.

question that arises then is: Why is a pyramidalized singlet state of $[CpFeH_2]^-$ not favored, as one would expect from the small HOMO/LUMO gap of the pseudo-C_{2v} conformation? The answer lies in the localization of the HOMO and LUMO. Indeed, perturbational theory states that the interaction between two orbitals upon perturbation depends on two independent factors: their energy difference and their overlap after perturbation.[1] It turns out that the HOMO and LUMO of the pseudo-C_{2v} $[CpFeH_2]^-$ have almost no hydrogen participation (3% and 1%, respectively). Consequently, they cannot overlap significantly upon pyramidalization since, being simply a hydride displacement, this distortion could only provide M−H overlap variation. In other words, being essentially CpFe localized, the HOMO and the LUMO remain almost unchanged when the hydrides move. As a result, the HOMO−LUMO gap hardly changes upon pyramidalization, the corresponding potential energy surface of the singlet state is flat, and the triplet state, of pseudo-C_{2v} symmetry (Table 1), is more stable by 0.60 eV. One of the reasons for the very small hydride participation in the HOMO and the LUMO of $[CpFeH_2]^-$ comes from the fact that hydrides are pure σ-donor ligands. Indeed, d-type levels tend to mix primarily with ligand π-type frontier orbitals.[1]

Replacing the hydride ligands in $[CpFeH_2]^-$ by monodentate phosphines pyramidalizes the singlet state, as shown by our calculations on $[CpFe(PH_3)_2]^+$ (Table 1), which lead to results similar to those obtained for $[CpFe(dpe)]^+$. Assuming the pseudo-C_{2v} geometry, the HOMO−LUMO gap of the singlet state of $[CpFe(PH_3)_2]^+$ is 0.29 eV and the phosphorus participation in these orbitals is 3% and 15%, respectively. These latter values are somewhat larger than in the case of L = H^-. This is why pyramidalization of the low spin is favored, but still the potential energy surface of the singlet state is rather flat and the pseudo-C_{2v} triplet state is the most stable by 0.14 eV.

Calculations on the $[CpFe(CO)_2]^+$ model lead to somewhat different results. The HOMO−LUMO gap calculated for the constrained pseudo-C_{2v} geometry is 0.44 eV, and the carbon participation in these orbitals is 4% and 11%, respectively. These values are not that much different than those found for the diphosphine model. However, the second-order Jahn−Teller instability of the pseudo-C_{2v} structure is larger since the pyramidalized low spin is stabilized to such an extent that it becomes the ground state (Table 1), contrary to the cases of $[CpFe(dpe)]^+$, $[CpFe(PH_3)_2]^+$, and $[CpFeH_2]^-$, for which the triplet state is the most stable. Our results on $[CpFe(CO)_2]^+$ are slightly different from those found by Harris and co-workers, on $[CpMn(CO)_2]$ at the DFT and CASSCF-PT2 levels, who found the triplet state favored by 0.3−0.4 eV.[17] However, the opposite result was found at the MP2 level, as well as for all their calculations on $[CpMn(CO)_2]$.

We have also investigated the electronic structure of 16-electron $CpML_2$ systems in the case where L is a π-donor ligand. The [CpRu(acac)] compound was chosen as a model for [Cp*Ru(acac)] (acac = OMeC(O)C(H)C(O)Me), which, although dimerized in the solid state, has been shown to be a true 16-electron species in solution.[4] We have also calculated $[CpCo(acac)]^+$ as a model for the hypothetical oxidized form of the 17-electron [Cp*Co(acac)] complex, which has been isolated and fully characterized in the solid state.[5] As predicted from earlier works,[13c,15b] [CpRu(acac)] and $[CpCo(acac)]^+$ are not pyramidalized in the singlet state (Table 1). Moreover, contrary to all the other computed 16-electron models, there is a strong energy preference for the low-spin configuration. This is due to the large HOMO−LUMO gap of these compounds (1.78 and 1.17 eV, respectively), which prevents them from pyramidalization. The existence of this large gap originates from the π-donor effect of the acac ligand, which destabilizes preferentially the b_1 LUMO of Figure 1. In the case of an 18-electron [CpM(acac)] species, this destabilization tends to reduce the HOMO(b_1)−LUMO(b_2) gap (see below).

Eighteen- and 17-Electron Species. Complexes of the $CpML_2$ type satisfying the 18-electron rule, such as $[CpCo(CO)_2]$, are well-known,[1,25] and their electronic structure has been described in detail.[1,13a,25b] As discussed above, they adopt the pseudo-C_{2v} geometry, which is expected to provide the molecule with a large HOMO−LUMO gap. This suggests that the presence of σ-donor or π-acceptor ligands favors diamagnetism. Interestingly, π-donor ligands such as acac seem to induce paramagnetism, as shown by the work of Andersen and co-workers, who recently synthesized and characterized the paramagnetic 18-electron [Cp*Ni(acac)] complex.[5] The X-ray crystal structure of [Cp*Ni(acac)] indicates a pseudo-C_{2v} geometry, as does that of the related 17-electron [Cp*Co(acac)] complex (see Table 1).[5]

To analyze this ligand effect, calculations were carried out on the [CpNi(acac)], [Cp*Ni(acac)], and [CpCo(acac)] models. The major results are reported in Table 1. The computed energy difference between the singlet and triplet states of [CpNi(acac)] is found to be very small (0.005 eV), a value not significantly different from 0 at the considered level of theory. Replacing Cp by Cp* tends to slightly favor a high-spin ground state (by 0.08 eV). These results are fully consistent with the observance above 150 K of a temperature-dependent spin-equilibrium for [Cp*Ni(acac)].[5] The differences between the singlet and triplet optimized geometries are quite small. In all cases the acac ligand is perfectly planar. Both singlet and triplet states adopt a close-to-C_{2v} conformation (Table 1). Overall, the experimental structure of [Cp*Ni(acac)] seems to look better like the singlet state geometry (see Table 1), but the differences found between the optimized geometries of the two spin states are too small to conclude.

The near degeneracy of the two spin states originates mainly from the destabilizing effect of the acac ligand on the b_1 HOMO (see above), inducing a small HOMO−LUMO gap which favors the occupation of the b_2 LUMO in the high-spin configuration. This gap is computed to be 0.59 eV for the optimized low-spin geometry of [CpNi(acac)]. It is reduced to 0.05 eV when the singlet state is computed on the triplet optimized geometry. As expected, no pyramidalization effect is calculated for both spin states. As said above in the case of $[CpFe(dpe)]^-$, the occupation of the b_2 LUMO in the triplet state has no effect on the pyramidalization driving force. The partial occupation of the b_1 HOMO is also ineffective, because of the large gap below this level (see below

the discussion on $[CpCo(acac)]^+$). For similar reasons, the 17-electron [CpCo(acac)] model is found also to adopt a pseudo-C_{2v} geometry close to the experimental structure of [Cp*Co(acac)].[5]

Calculations were also carried out on the 18-electron $[CpNiCl_2]^-$ model, in which no chelating effect is present, allowing the energy of the frontier orbitals to vary within the pseudo-C_{2v} symmetry through variation of the L−M−L angle. As shown by the results reported in Table 1, the triplet state is stabilized by a large Cl−Ni−Cl angle, which lowers the b_2 MO by reducing its Ni−Cl antibonding character.

The $[CpFe(dpe)(H_2O)]^+$, $[CpFe(dpe)(OCMe_2)]^+$, and $[CpFe(dpe)(OSO_2CF_3)]$ Series

Three 18-electron complexes that can be described as resulting from the assembly of the $[Cp^*Fe(dppe)]^+$ unit with a 2-electron oxygen-containing ligand have been structurally characterized in the solid state: $[Cp^*Fe(dppe)(H_2O)]^+$, $[Cp^*Fe(dppe)(OCMe_2)]^+$, and $[Cp^*Fe(dppe)(OSO_2CF_3)]$.[6f,18] The peculiarity of this class of compounds originates from the fact that they have been shown to exhibit paramagnetic behavior. THF solutions of the three complexes are paramagnetic. However, these complexes are partly dissociated in solution. Consequently, it is difficult to assess the part of the magnetic signal originating from the undissociated 18-electron species with respect to that of the 16-electron $[Cp^*Fe(dppe)]^+$ species. In the solid state, $[Cp^*Fe(dppe)(H_2O)]^+$ is diamagnetic, at least in the form of the salt of PF_6^-.[6f] On the other hand, $[Cp^*Fe(dppe)(OCMe_2)]^+$ and $[Cp^*Fe(dppe)(OSO_2CF_3)]$ have been shown to be paramagnetic in the solid state.[6f,18] SQUID measurements on the former lead to $\mu_{eff} = 2.90\ \mu_B$ in the range 77−310 K,[18a] while on the latter an antiferromagnetic behavior was found, with a singlet−triplet separation lower than 20 cm^{-1} (0.002 eV).[18b] The related complexes $[CpFe(dippe)(MeCN)]^+$ and $[Cp^*Fe(dippe)(MeCN)]^+$ have been shown to be diamagnetic and paramagnetic, respectively.[9b] Although these behaviors have been recorded in solution, they may not originate from MeCN dissociation.[9b] Similarly, $[CpFe(dppe)(OCMe_2)]^+$ is likely to be diamagnetic in solution,[18a] while, as said above, its Cp* relative is paramagnetic.

DFT calculations were carried out on the models $[CpFe(dpe)(H_2O)]^+$, $[CpFe(dpe)(OCMe_2)]^+$, and $[CpFe(dpe)(OSO_2CF_3)]$. The optimized geometries are shown in Figure 3. The major metrical data are reported in Table 2, together with some X-ray data concerning $[Cp^*Fe(dppe)(H_2O)]^+$, $[Cp^*Fe(dppe)(OCMe_2)]^+$, and $[Cp^*Fe(dppe)(OSO_2CF_3)]$.[6f,18]

The optimized structures of the singlet and triplet states of $[CpFe(dpe)(H_2O)]^+$ are shown in Figure 3a,b. Their main difference lies in the conformation of the H_2O ligand. In the high-spin case, the coordination of the oxygen atom is planar and the H_2OFe plane is perpendicular to the Cp ring. This conformation allows a three-electron stabilization between the oxygen π-lone pair and the occupied π-type frontier orbital of the $[CpFe(dpe)]^+$ fragment which is perpendicular to the Cp ring. In the low-spin case, the three-electron stabilization is changed into a four-electron repulsion. To minimize this repulsion, the oxygen lone pair rotates in such a way that it interacts now with the other π-type

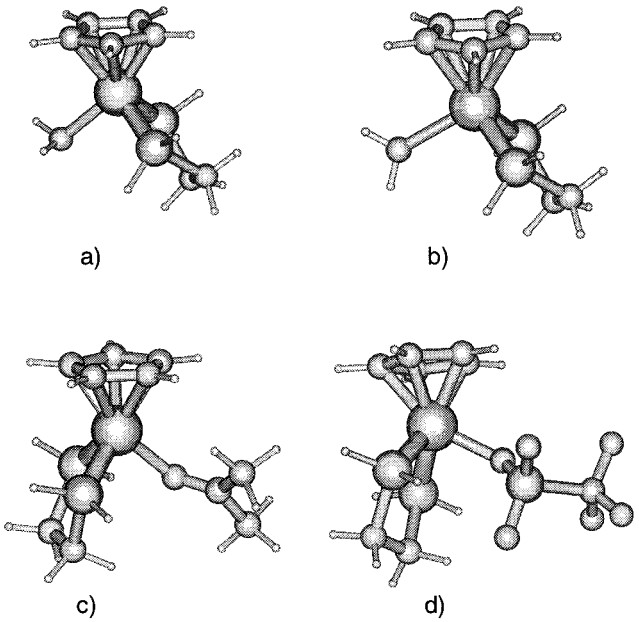

Figure 3. Optimized geometries of (a) $[CpFe(dpe)(H_2O)]^+$ ($S = 0$); (b) $[CpFe(dpe)(H_2O)]^+$ ($S = 1$); (c) $[CpFe(dpe)(OCMe_2)]^+$ ($S = 0$); and (d) $[CpFe(dpe)(OSO_2CF_3)]$ ($S = 0$). Plots were obtained by using the MOLDEN package (Schaftenaar, G., CAOS/CAMM Center Nijmegen, The Netherlands).

orbital of $[CpFe(dpe)]^+$, which is less hybridized and provides a smaller overlap. The oxygen pyramidalization tends also to minimize this overlap. This difference of the Fe−O π-type interaction in the singlet and triplet states of $[CpFe(dpe)(H_2O)]^+$ is illustrated in Figure 4. Unfortunately, the X-ray structure of $[Cp^*Fe(dppe)(H_2O)]^+$, which found the orientation of the H_2O ligand intermediate between those of Figure 4,[18b] is not accurate with repect to the position of the hydrogen atoms. Comparison of the other experimental distances of $[Cp^*Fe(dppe)(H_2O)]^+$ with the optimized structures of $[CpFe(dpe)(H_2O)]^+$ indicates a better consistency with the singlet state structure, except for the Cp(centroid)−Fe−O angle (Table 1). The singlet state of $[CpFe(dpe)(H_2O)]^+$ is computed to be the most stable by 0.59 eV. Single-point calculations performed on $[CpFe(dpe)(H_2O)]^+$ and assuming a molecular geometry derived from the X-ray structure of $[Cp^*Fe(dppe)(H_2O)]^+$ found also the singlet state to be more stable by 0.90 eV.

Calculations on the $[CpFe(dpe)(OCMe_2)]^+$ model for both spin states lead to optimized conformations and geometrical features which are both quite similar to the X-ray structure $[Cp^*Fe(dppe)(OCMe_2)]^+$ (Figure 3d and Table 2). In these systems, the orientation of the acetone ligand with respect to the metallic unit is partly dictated by steric factors. The optimized Fe−O distance of the singlet state is closer to the experimental value than the corresponding triplet optimized distance. On the other hand, the triplet Cp(centroid)−Fe−O and Fe−O−C angles are closer to the experimental values. The optimized singlet state is computed to be 0.72 eV more stable than the triplet one. Single-point calculations performed on $[CpFe(dpe)(OCMe_2)]^+$ and assuming a molecular geometry derived from the X-ray structure of $[Cp^*Fe(dppe)(OCMe_2)]^+$ found also the singlet state to be more stable by 0.97 eV. As for the acetone complex, the singlet and triplet optimized geometries of [CpFe-

Table 2. Major Experimental and Optimized Structural Data and Relative Energies for $CpML_2(X)$ Species ($X = OH_2$, OCMe2, OSO_2CF_3)

		Fe−C (Å) average (range)	Fe−P (Å)	Fe−O (Å)	P−Fe−P (deg)	C′−Fe−O (deg)[a]	P−Fe−O (deg)	α (deg)	energy (eV)
$[\{CpFe(dpe)\}(OH_2)]^+$	expt[b]	2.11 (2.08−2.13)	2.23, 2.22	2.06	85	120	87, 90	153	0.92 (S)[c]
	S	2.12 (2.09−2.14)	2.23, 2.21	2.12	85	130	92, 89	139	0.00
	T	2.24 (2.17−2.27)	2.29, 2.25	2.30	84	118	98, 98	141	0.59
$[\{CpFe(dpe)\}(OCMe_2)]^+$	expt[d]	2.11 (2.10−2.12)	2.28, 2.23	2.03	85	122	84, 90	152	0.94 (S)[c]
	S	2.12 (2.10−2.14)	2.23, 2.21	2.03	85	130	82, 90	145	0.00
	T	2.24 (2.18−2.28)	2.28, 2.26	2.26	83	125	84, 88	149	0.72
$[\{Cp^*Fe(dpe)\}(OCMe_2)]^+$	S	2.13 (2.12−2.14)	2.24, 2.22	2.05	84	124	83, 93	148	0.00
	T	2.24 (2.16−2.31)	2.29, 2.29	2.26	83	123	88, 87	150	0.68
$[\{Cp^*Fe(dppe)\}(OCMe_2)]^+$	S	2.15 (2.14−2.17)	2.28, 2.24	2.04	86	122	91, 84	151	0.00
	T	2.26 (2.20−2.31)	2.29, 2.33	2.19	84	121	88, 88	151	0.53
$[\{CpFe(dpe)\}(OSO_2CF_3)]$	expt[e]	2.12 (2.10−2.14)	2.26, 2.25	2.13	84	118	83, 95	153	1.35 (S)[c]
	S	2.11 (2.10−2.12)	2.21, 2.21	2.05	86	121	82, 97	149	0.00
	T	2.25 (2.17−2.28)	2.31, 2.23	2.16	83	113	86, 97	153	0.72

[a] C′ = Cp and Cp* centroid. [b] X-ray structure of $[Cp^*Fe(dppe)(OH_2)]^+$ (from ref 6f). [c] Single-point calculation (ground state) performed on the X-ray structure in which the methyl and phenyl groups were replaced by hydrogen atoms (C−H = 1.09 Å; P−H = 1.42 Å). [d] X-ray structure of $[Cp^*Fe(dppe)(OCMe_2)]^+$ (from ref 17a). [e] X-ray structure of $[Cp^*Fe(dppe)(OSO_2CF_3)]$ (from ref 6f).

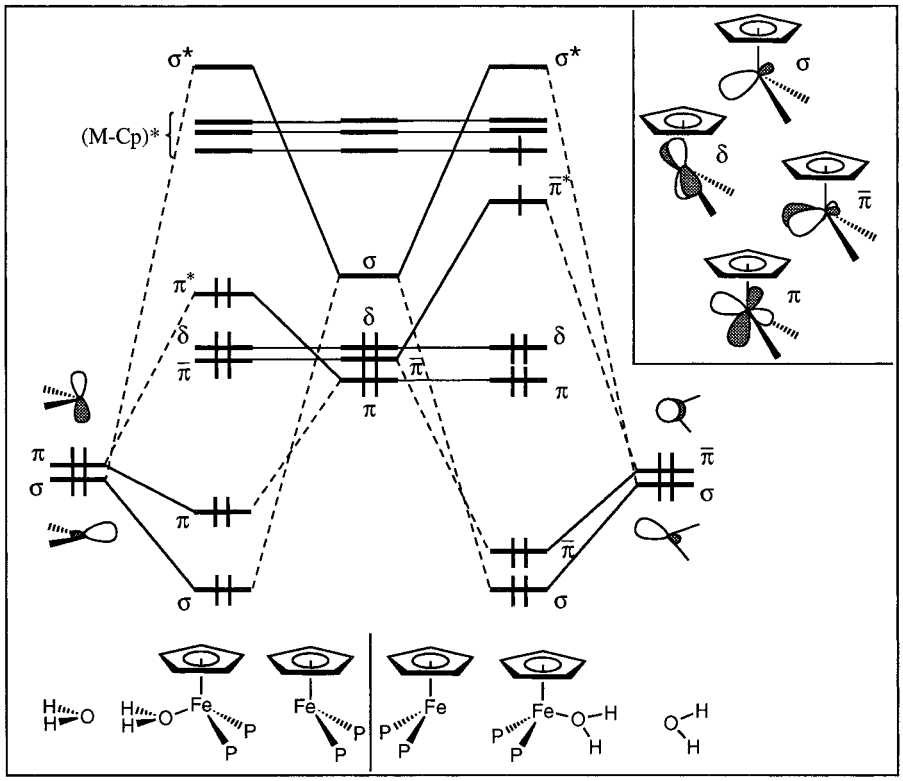

Figure 4. Qualitative MO interaction diagram between H_2O and $[CpFe(dpe)]^+$ in the complex $[CpFe(dpe)(H_2O)]^+$. Left: singlet state. Right: triplet state. The frontier orbitals of the $[CpFe(dpe)]^+$ fragment are sketched in the upper right corner.

$(dpe)(OSO_2CF_3)]$ are quite similar and resemble the X-ray structure of $[Cp^*Fe(dppe)(OSO_2CF_3)]$ (Figure 3c and Table 2). The optimized singlet state is found to be 0.72 eV more stable than the triplet state. A similar result is found (0.77 eV) when single-point calculations are performed on this molecule, assuming a molecular geometry derived from the X-ray structure of $[Cp^*Fe(dppe)(OSO_2CF_3)]$.

The singlet−triplet separations computed on the 18-electron $[CpFe(dpe)(OCMe_2)]^+$ and $[CpFe(dpe)(OSO_2CF_3)]$ models are too large to account for the magnetism of $[Cp^*Fe(dppe)(OCMe_2)]^+$ and $[Cp^*Fe(dppe)(OSO_2CF_3)]$. Experiments in solution suggest that the use of a simple Cp ligand instead of a methylated Cp* in the complexes of acetone and acetonitrile leads to diamagnetic systems.[9b,10a,d,11] To evaluate the effect of substituting Cp* by Cp and dppe by dpe, we have also performed full geometry optimizations on $[Cp^*Fe(dpe)(OCMe_2)]^+$ and $[Cp^*Fe(dppe)(OCMe_2)]^+$ (see Table 2). The results are quite similar to those obtained for the simplified model $[CpFe(dpe)(OCMe_2)]^+$. The singlet−triplet separation is slightly reduced in the Cp* models, but not enough to account for the magnetic behavior of $[Cp^*Fe(dppe)(OCMe_2)]^+$.

Conclusion

The question of the spin state, geometry, and structural dynamics of $CpML_2$ 16-electron complexes is related to the second-order Jahn−Teller instability of their pseudo-C_{2v} geometry. Such an instability depends on two factors: (i) the HOMO (a_1)−LUMO (b_1) gap

(ΔE_{HL}); the smaller the ΔE_{HL}, the more unstable the pseudo-C_{2v} geometry with respect to pyramidalization; (ii) the HOMO−LUMO overlap (S_{HL}) when pyramidalization is applied; the larger the S_{HL}, the more unstable the pseudo-C_{2v} structure. In the case where L = H^- (pure σ-donor ligand), our DFT investigations show that, unlike EHT calculations, ΔE_{HL} is small. However, the HOMO and LUMO cannot overlap significantly upon pyramidalization. As a consequence, the Jahn−Teller instability of the pseudo-C_{2v} geometry is weak, resulting in a pseudo-C_{2v} singlet state with a flat potential energy surface associated with its pyramidalization. Another consequence of the small ΔE_{HL} and S_{HL} values is that the triplet state is the ground state. When L is a π-acceptor ligand, ΔE_{HL} remains small, but S_{HL} is somewhat larger. This situation tends to slightly stabilize the singlet state in its pyramidalized form. The resulting singlet−triplet energy separation is small (computed to be less than 0.15 eV in the gas phase). Whith the weak π-acceptor phosphine ligands, the triplet state is the ground state, while with the strong π-acceptor CO ligand the singlet state is the most stable. When L is a π-donor ligand, the b_1 LUMO is strongly destabilized, leading to a large ΔE_{HL} value. As a result, the pseudo-C_{2v} structure is favored, with a singlet ground state. The weak singlet/triplet separation existing in the case where L is not a strong π-donor may favor spin interconversion and in turn play some role in the reactivity of these unsaturated species.[26]

In the case of 18-electron $CpML_2$ species, this b_1 level is the HOMO. Its destabilization by π-donor ligands such as acac results in a small HOMO (b_1)−LUMO (b_2) gap, favoring a low-energy triplet state. Calculations on the 18-electron [CpNi(acac)] model found nearly degenerate singlet and triplet states. All the computed 17-electron $CpML_2$ models were found to adopt a structure intermediate between their 16-electron and 18-electron parents in their singlet states.

A series of neutral and cationic 18-electron complexes of the general type $CpFeL_2L'$, in which L′ is a ligand bonded to the metal through an Fe−O bond, have also been investigated. Although the existence of an Fe−O bond induces the presence of a rather low-lying σ*(Fe−O) LUMO, the lowest triplet state is not calculated to be the ground state, and calculations on all the considered models are consistent with a diamagnetic behavior. Unlike for the 16−18-electron $CpML_2$ series, there is no full agreement in this family between calculations and reported magnetic behavior. Contradiction with experiment is found for $[Cp^*Fe(dppe)(OCMe_2)]^+$ and $[CpFe^*(dppe)(OSO_2CF_3)]$, which are reported to be paramagnetic. Clearly, more experimental data are needed in these series of compounds in order to understand this unconsistency, which may be attributable to either solvent, ionic, or crystal interactions in these polar molecules, but which are not taken into account in these calculations.

Acknowledgment. Drs. J.-R. Hamon, C. Lapinte, and J.-F. Halet are acknowledged for their interactive interest during the progress of this work and for their numerous helpful comments. Calculations were performed at the Centre de Ressources Informatiques (CRI) of Rennes and the Institut de Développement et de Ressources en Informatique Scientifique (IDRIS-CNRS) of Orsay.

OM990191I

(26) Detrich, J. L.; Reinaud, O. M.; Rheingold, L. R.; Theopold, K. H. *J. Am. Chem. Soc.* **1995**, *117*, 11745.